

# The $\gamma p \rightarrow \pi^+ n$ Single Charged Pion Photoproduction.

W. Chen, D. Dutta (co-spokesperson, contact person), H. Gao (co-spokesperson)

K. Kramer, X. Qian, Q. Ye, X. F. Zhu, X. Zong

*Triangle Universities Nuclear Lab, Duke University and*

*Department of Physics, Duke University, Durham, NC 27708*

E. De Sanctis, M. Mirazita, S.A. Pereira, F. Ronchetti, P. Rossi (co-spokesperson)

*INFN, Laboratori Nazionali di Frascati*

M. Battaglieri, R. De Vita

*INFN, sezione di Genova*

W. J. Briscoe, I. I. Strakovsky

*George Washington University*

A. Deppman, J. de Oliveira Echeimberg

*Universidade de São Paulo, São Paulo, Brasil*

and the **CLAS Collaboration**

PACS numbers:

Exclusive  $\gamma N \rightarrow \pi N$  processes are essential probes to study the transition from meson-nucleon degrees of freedom to quark-gluon degrees of freedom. One of the simplest signatures for this transition is the scaling of the cross-section with center-of-mass energy. The cross sections of these processes are also advantageous, for investigation of the possible oscillatory behavior around the quark counting prediction, since they decrease relatively slower with energy compared with other photon-induced processes. In addition to this, recent data from JLab experiment E94-104 show dramatic change in the scaled differential cross-section from the  $\gamma n \rightarrow \pi^- p$  and  $\gamma p \rightarrow \pi^+ n$  processes in the center of mass energy between 1.8 GeV to about 2.4 GeV. We propose to perform  $\gamma p \rightarrow \pi^+ n$  measurement from hydrogen in Hall B using the CLAS detector, for photon energies between 2.0 to 5.4 GeV. CLAS has the distinct advantage of permitting a much finer energy scan and simultaneous coverage of a large angular range, which will help investigate the dramatic behavior observed in experiment E94-104. It will also help confirm the possibility of oscillations in the scaled differential cross-section at large C. M. angles. The proposed experiment requires 100 hours ( $\approx 4$  days) of CW

electron beam at  $E_0 = 5.7$  GeV with 25 nA current on a 40 cm liquid hydrogen target.

## INTRODUCTION

The interplay between the nucleonic and partonic pictures of the strong interaction represents one of the major issues in contemporary nuclear physics. Although standard nuclear models are successful in describing the interactions between hadrons at large distances, and Quantum Chromodynamics (QCD) accounts well for the quark interactions at short distances, the physics connecting the two regimes remains unclear. In fact, the classical nucleonic description must break down once the probing distances become comparable to those separating the quarks. The challenge is to study this transition region by looking for the onset of some experimentally accessible phenomena naturally predicted by perturbative QCD (pQCD). The simplest is the constituent counting rule (CCR) for high energy exclusive reactions [1], in which  $d\sigma/dt \propto s^{-n+2}$ , with  $n$  the total number of point-like particles and gauge fields in the initial plus final states. Here  $s$  and  $t$  are the invariant Mandelstam variables for the total energy squared and the four-momentum transfer squared, respectively. Many exclusive reactions [2] at high energy and large momentum transfer appear to obey the CCR and in recent years, a similar trend, i.e. global scaling behavior, has been observed in deuteron photo-disintegration experiments [3] - [6] and in photo-production of charged pions [7] at a surprisingly low transverse momentum value of  $\sim 1.1$  (GeV/c)<sup>2</sup>.

The same dimensional analysis which predicts the quark counting rule also predicts hadron helicity conservation for exclusive processes at high energy and large momentum transfers. However, polarization measurements on deuteron photo-disintegration [8], recently carried out in Hall A at Jefferson Lab (JLab), show disagreement with hadron helicity conservation in the same kinematic region where the quark counting behavior is apparently observed. These paradoxes make it essential to understand the exact mechanism governing the early onset of scaling behavior.

Towards this goal, it is important to look closely at claims of agreement between the differential cross section data and the quark counting prediction. Historically, the elastic proton-proton ( $pp$ ) scattering at high energy and large momentum transfer has played a very important role. In fact, the re-scaled 90° center-of-mass  $pp$  elastic scattering data,  $s^{10} \frac{d\sigma}{dt}$  show substantial oscillations about the power law behavior. Oscillations are not restricted

to the  $pp$  sector; they are also seen in  $\pi p$  fixed angle scattering [9, 10]. The old [11] as well as the new data from JLab experiment E94-104 on photo-production of charged pions at  $\theta_{cms} = 90^\circ$  [7] also show hints of oscillation about the  $s^{-7}$  scaling (see Fig. 1). Thus, it is essential to confirm and map out these oscillatory scaling behavior.

Beside the interest in looking for the onset of phenomena predicted by the pQCD, the study of the charged pions photo-production has also other appealing features. In fact, by looking at Fig. 1 the data below the scaling region show an interesting enhancement at a center-of-mass energy ranging approximately from 1.8 GeV to 2.5 GeV. This enhancement was seen in both channels of the charged pion photoproduction. One also notes a very striking feature from the data i.e. the scaled differential cross-section dropped by a factor of several units in a very narrow windows of the center of mass energy ( $\sim 200$ - $300$  MeV). Using high luminosity experimental facilities such as CEBAF, the oscillatory scaling behavior as well as the apparent enhancement and rapid fall-off below the scaling region can be investigated with significantly improved precision. This will help us to identify the exact nature and the underlying mechanism responsible for the scaling behavior and to reveal the nature of the observed enhancement.

In this experiment, we propose to measure the cross-section  $\frac{d\sigma}{dt}$  for the  $p(\gamma, \pi^+)n$  processes. In particular, we plan to map out the region of  $\sqrt{s} = 2.15 - 3.35$  GeV in fine energy bins and center-of-mass angular bins of  $10^\circ$ . The proposal body is organized as following. Section II contains the physics motivations for the measurement, in Section III the proposed measurement is described and results from a Monte Carlo simulations of the experiment are reported, Section IV contains details of the experiment, evaluation of the counting rates and the beam time request, and Section V is the summary.

## PHYSICS MOTIVATIONS

### Constituent Counting Rule and Oscillations

The constituent counting rule predicts the energy dependence of the differential cross section at fixed center-of-mass angle for an exclusive two-body reaction at high energy and large momentum transfer as follows:

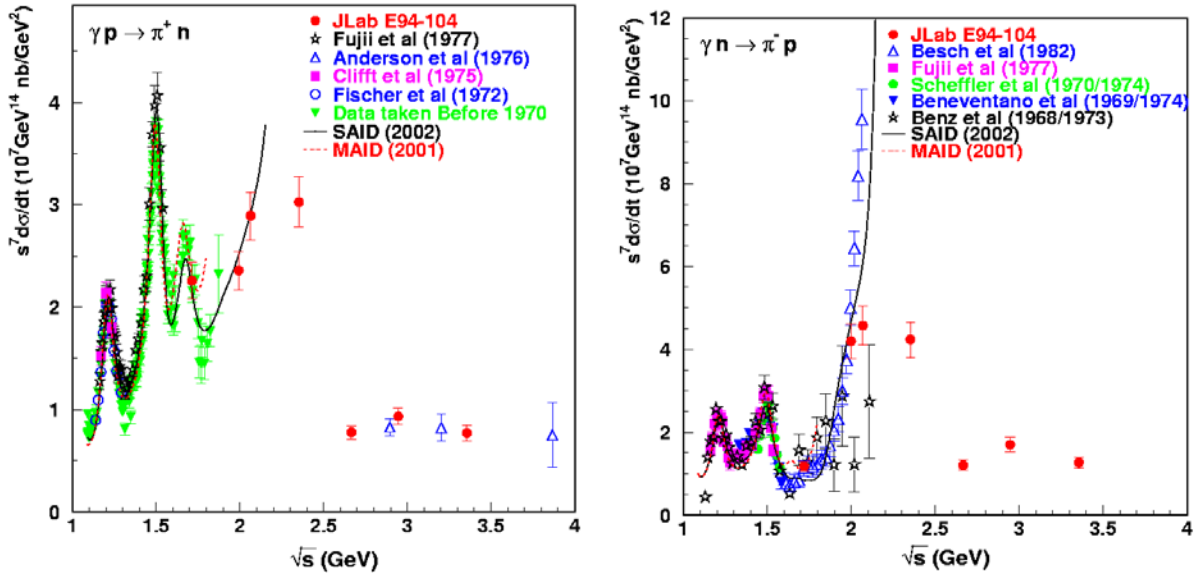


FIG. 1: The scaled differential cross section,  $s^7 \frac{d\sigma}{dt}$  as a function of  $\sqrt{s}$  at a center-of-mass angle of  $90^\circ$  for  $\gamma p \rightarrow \pi^+ n$  channel (left) and the  $\gamma n \rightarrow \pi^- p$  channel (right). The data from JLab E94-104 are shown as solid circles. The error bars for the new data and for the Anderson *et al.* data [11], include statistical and systematic uncertainties. Other data sets [9, 10] are shown with only statistical errors. The open squares (right panel) were averaged from data at  $\theta_{cm} = 85^\circ$  and  $95^\circ$  [12]. The solid line was obtained from the recent partial-wave analysis of single-pion photoproduction data [13] up to  $E_\gamma=2$  GeV, while the dashed line from the MAID analysis [14] up to  $E_\gamma=1.25$  GeV.

$$d\sigma/dt = h(\theta_{cm})/s^{n-2} \quad (1)$$

where  $s$  and  $t$  are the Mandelstam variables, respectively the square of the total energy in the center-of-mass frame and the momentum transfer squared. The quantity  $n$  is the total number of elementary fields in the initial and final states, while  $h(\theta_{cm})$  depends on details of the dynamics of the process.

The quark counting rule was originally obtained based on dimensional analysis under the assumptions that the only scales in the system are momenta and that composite hadrons can be replaced by point-like constituents. Implicit in these assumptions is the approximation that the class of diagrams which represent on-shell independent scattering of pairs of constituent quarks (Landshoff diagrams) [15], can be neglected. Also neglected were con-

tributions from quark orbital angular momentum which are power suppressed but can give rise to hadron helicity flipping amplitudes. Later on, these counting rules were confirmed within the framework of perturbative QCD analysis up to a logarithmic factor of  $\alpha_s$  and are believed to be valid at high energy in the perturbative QCD region. Such analysis relies on the factorization of the exclusive process into a hard scattering amplitude and a soft quark amplitude inside the hadron. Finally, in the last few years an all-orders demonstration of the counting rules for hard exclusive processes has been shown to arise from the correspondence between the anti-de Sitter space and conformal field theory [16] which connects superstring theory to superconformal gauge theory.

Although the quark counting rule agrees with data from a variety of exclusive processes, the other natural consequence of pQCD, i.e. the helicity conservation selection rule (HHC), tends not to agree with data in the experimentally tested region. HHC arises from the fact that vector interactions (photon or gluon coupling with quarks) conserve chirality, leading to conservation of the sum of the components of the hadronic spins along their respective momentum directions, and of predictions of spin observables. In deriving this rule, higher orbital angular momentum states of quarks or gluons in hadrons are neglected.

If hadron helicity conservation holds, the induced polarization of the recoil proton in the unpolarized deuteron photo-disintegration process is expected to be zero. A polarization measurement [8] in deuteron photo-disintegration has been carried out recently by the JLab E89-019 collaboration. While the induced polarization does seem to approach zero around a photon energy of 1.0 GeV at  $90^\circ$  center-of-mass angle, the polarization transfer data are inconsistent with hadron helicity conservation.

Thus the entire subject is very controversial and there are no definitive answers to the question- *what is the energy threshold at which pQCD can be applied?*

Indeed, Isgur and Llewellyn-Smith [17] argue that if the nucleon wave-function has significant strength at low transverse quark momenta ( $k_\perp$ ), then the hard gluon exchange (essential to the perturbative approach) which redistributes the transferred momentum among the quarks, is no longer required and the applicability of perturbative techniques at these low momentum transfers is in serious question. Indeed the exact mechanism governing the observed quark counting rule behavior remains a mystery. Thus, it is crucial to deeply investigate the CCR and HHC and also look for other pQCD signatures.

To this end the elastic proton-proton ( $pp$ ) scattering at high energy and large momentum

transfer has played a very important role. First, a deeply investigation of the differential cross section of this process shows oscillations about the scaling behavior  $s^{-10}$  predicted by the quark counting rule [18]. Secondly, the spin correlation experiment in  $pp$  scattering first carried out at Argonne by Crabb *et al.* [19] shows striking behavior: at the largest momentum transfers ( $p_T^2 = 5.09 \text{ (GeV/c)}^2$ ,  $\theta_{c.m.} = 90^\circ$ ) it is  $\sim 4$  times more likely for protons to scatter when their spins are both parallel and normal to the scattering plane than when they are anti-parallel. Later spin-correlation experiments [20] confirm the early observation by Crabb *et al.* and showed that the spin correlation  $A_{NN}$  (given by  $\frac{\sigma(\uparrow,\uparrow)-\sigma(\uparrow,\downarrow)}{\sigma(\uparrow,\uparrow)+\sigma(\uparrow,\downarrow)}$ ) varies with energy about the pQCD prediction.

Theoretical interpretation of this oscillatory behavior of the scaled cross-section ( $s^{10} \frac{d\sigma}{dt}$ ) and the striking spin-correlation in  $pp$  scattering was attempted by many authors. Some explained these features as the result of the interference between hard pQCD short-distance and long-distance (Landshoff) amplitudes [21], [22], [23]; others as the opening of a  $c\bar{c}uudud$  resonant states [24].

Very recently, a number of new developments have generated renewed interest in this topic. Zhao and Close [25] have argued that a breakdown in the locality of quark-hadron duality (dubbed as “restricted locality” of quark-hadron duality) results in oscillations around the scaling curves predicted by the counting rule. They explain that the smooth behavior of the scaling laws arise due destructive interference between various intermediate resonance states in exclusive processes at high energies, however at lower energies this cancellation due to destructive interference breaks down locally and gives rise to oscillations about the smooth behavior. On the other hand, Ji *et al.* [26] have derived a generalized counting rule based on pQCD analysis, by systematically enumerating the Fock components of a hadronic light-cone wave function. Their generalized counting rule for hard exclusive processes include parton orbital angular momentum and hadron helicity flip, thus they provide the scaling behavior of the helicity flipping amplitudes. The interference between the different helicity flip and non-flip amplitudes offers a new mechanism to explain the oscillations in the scaling cross-sections and spin correlations. Brodsky *et al.* [27] have used the anti-de Sitter/Conformal Field Theory correspondence or string/gauge duality [16] to compute the hadronic light front wave functions exactly and it yields an equivalent generalized counting rule without the use of perturbative theory.

It was previously thought that the oscillatory  $s^{10} \frac{d\sigma}{dt}$  feature is unique to  $pp$  scattering

or to hadron induced exclusive processes. However, it has been suggested that similar oscillations should occur in deuteron photo-disintegration [28], and photo-pion productions at large angles [29]. The QCD re-scattering calculation of the deuteron photo-disintegration process by Frankfurt, Miller, Sargsian and Strikman [28] predicts that the additional energy dependence of the differential cross-section, beyond the  $s^{11} \frac{d\sigma}{dt}$  scaling arises primarily from the  $n - p$  scattering in the final state. If these predictions are correct, such oscillatory behavior may be a general feature of high energy exclusive photoreactions. Thus it is very important to experimentally search for these oscillations in photoreactions.

Farrar, Sterman and Zhang [30] have shown that the Landshoff contributions are suppressed at leading-order in large-angle photoproduction but they can contribute at subleading order in  $\frac{1}{Q}$  as pointed out by the same authors. In principle, the fluctuation of a photon into a  $q\bar{q}$  in the initial state can also contribute to an independent scattering amplitude at sub-leading order. However, the vector-meson dominance diffractive mechanism is already suppressed in vector meson photoproduction at large values of  $t$  [31]. On the other hand such independent scattering amplitude can contribute in the final state if more than one hadron exist in the final state, which is the case for both the deuteron photo-disintegration and nucleon photo-pion production reactions. Thus, an unambiguous observation of such an oscillatory behavior in exclusive photoreactions with hadrons in the final state at large  $t$  may provide a signature of QCD final state interaction. The most recent data on  $d(\gamma, p)n$  reaction [5, 6] show that the oscillations, if present, are very weak in this process, and the rapid drop of the cross section ( $\frac{d\sigma}{dt} \propto \frac{1}{s^{11}}$ ) makes it impractical to investigate such oscillatory behavior.

Given that the nucleon photo-pion production has a much larger cross-section at high energies ( $\frac{d\sigma}{dt} \propto \frac{1}{s^7}$ ), it is very desirable to use these reactions to verify the existence of such oscillations. In fact some precision data on  $\gamma p \rightarrow \pi^+ n$  and  $\gamma n \rightarrow \pi^- p$  was recently reported by JLab experiment E94-104 [7]. The results (Fig. 1) indicate the constituent counting rule behavior at center-of-mass angle of  $90^\circ$ , for photon energies above  $\sim 3$  GeV (i.e. above the resonance region). In addition to the  $s^{-7}$  scaling behavior, these data also suggest an oscillatory behavior. However, the rather coarse beam energy settings prevent a conclusive statement about the oscillatory behavior. Thus, to verify any structure in the scaled cross-section of photo-pion production processes, it is imperative that we do a fine scan of the scaling region for the  $\gamma p \rightarrow \pi^+ n$  and  $\gamma n \rightarrow \pi^- p$  processes. The relatively higher rates

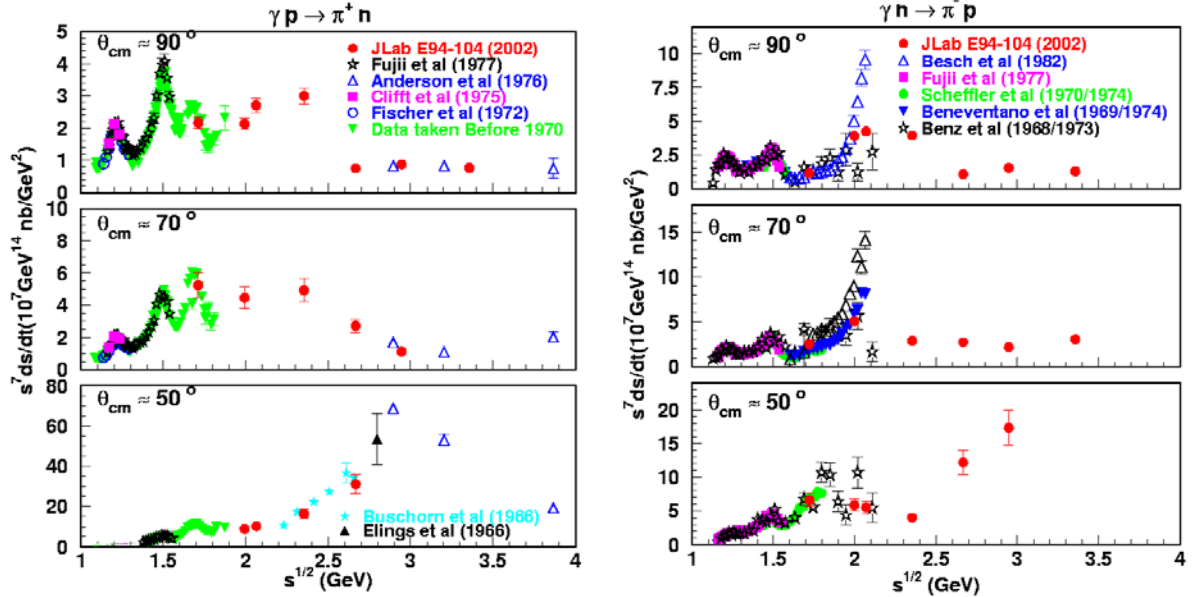


FIG. 2: The scaled differential cross section  $s^7 \frac{d\sigma}{dt}$  versus center-of-mass energy for the  $\gamma p \rightarrow \pi^+ n$  at  $\theta_{cm} = 90^\circ, 70^\circ, 50^\circ$  (left). And the scaled differential cross section  $s^7 \frac{d\sigma}{dt}$  versus center-of-mass energy for the  $\gamma n \rightarrow \pi^- p$  at  $\theta_{cm} = 90^\circ, 70^\circ, 50^\circ$  (right).

for these processes will also allow angular scans to investigate the momentum transfer ( $t$ ) and transverse momentum ( $p_T$ ) dependence of the scaling behavior in addition to the usual energy scan looking at the center-of-mass energy ( $W = \sqrt{s}$ ) dependence.

### The Dramatic Enhancement and Rapid Drop Seen in E94-104 Data

Results from Experiment E94-104 carried out in Hall A at the JLab for single pion photoproduction are shown in Figure 1. They agree with the world data within uncertainties in the overlapping region. As mentioned earlier, the data at  $\theta_{cm} = 70^\circ, 90^\circ$  exhibit a global scaling behavior predicted by the constituent counting rule in both  $\pi^-$  and  $\pi^+$  channels. The data at  $\theta_{cm} = 50^\circ$  do not display scaling behavior and may require higher photon energies for the observation of the onset of the scaling behavior. The data suggest that a transverse momentum of around 1.2 GeV/c might be the scale governing the onset of scaling for the photo-pion production, which is consistent with what has been observed in deuteron photodisintegration [5, 6].

An interesting feature of the data is an apparent enhancement in the scaled differential

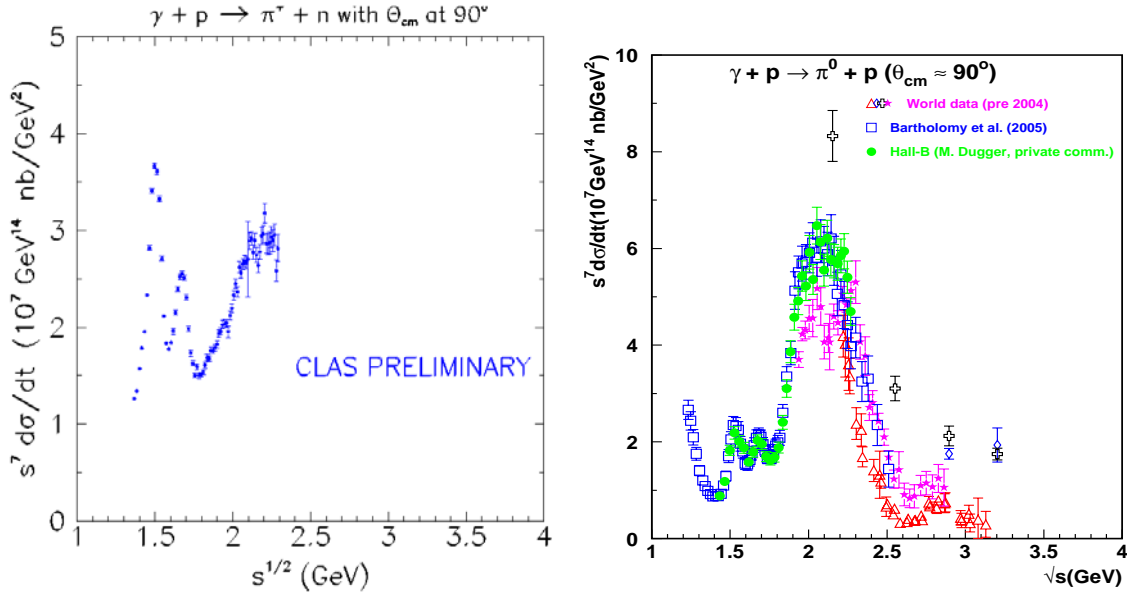


FIG. 3: Preliminary results from CLAS g1c on the scaled differential cross section  $s^7 \frac{d\sigma}{dt}$  versus center-of-mass energy for the  $\gamma p \rightarrow \pi^+ n$  at  $\theta_{cm} = 90^\circ$  (left). And preliminary results from CLAS on the scaled differential cross section  $s^7 \frac{d\sigma}{dt}$  versus center-of-mass energy for the  $\gamma p \rightarrow \pi^0 p$  at  $\theta_{cm} = 90^\circ$ , together with world data and the Bonn data (right).

cross section at center-of-mass angle of  $90^\circ$  below the scaling region, at a center-of-mass energy ranging approximately from 1.8 GeV to 2.5 GeV, followed by a rapid drop-off in a very narrow center-of-mass energy window. This feature is seen in both channels of the charged pion photoproduction, as shown in Fig. 2. This effect has been observed in existing neutral pion photoproduction [9, 10] data as well as in the preliminary CLAS results on the  $\gamma p \rightarrow \pi^+ n$  ( $\sqrt{s} \leq 2.3$  GeV only) and the  $\gamma p \rightarrow \pi^0 p$  channels shown in Fig. 3 [32, 33]. Without any conclusive statements at present, some speculations might be made. The observed enhancement around 2.2 GeV might relate to some unknown baryon resonances, as some of the well known baryon resonances ( $\Delta$ ,  $N^*$ 's around 1.5 GeV and 1.7 GeV) are clearly seen in the scaled cross section below 2.2 GeV. Several baryon resonances are predicted to be in this energy region by the constituent quark model [34], but have not been seen experimentally, i.e. the so called 'missing resonances'. The observed enhancement might be associated with the strangeness production threshold [24, 35]. They could also be related to the  $\phi$ -N bound state which has been predicted recently [36]. Thus a fine energy scan and a fine angular scan in the center-of-mass energy range of 1.8 - 2.5 GeV is urgently

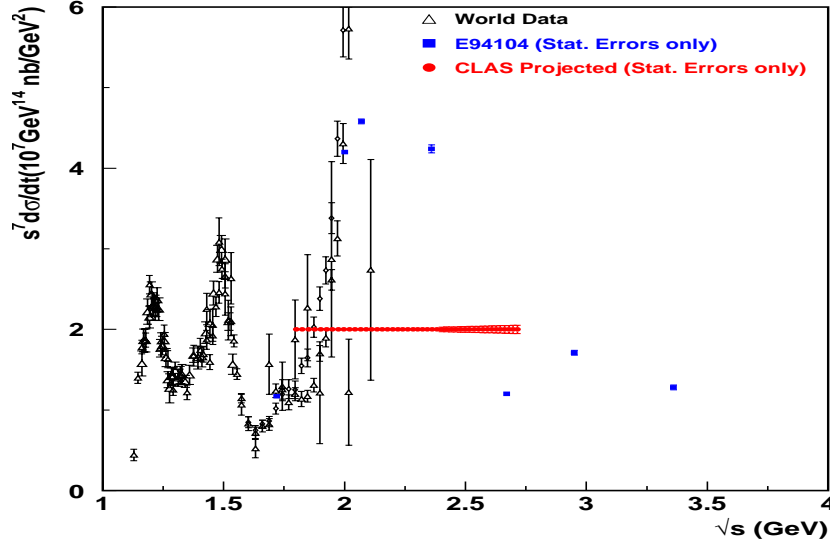


FIG. 4: Projected results for the  $\gamma n \rightarrow \pi^- p$  process at  $\theta_{cm} = 90^\circ$  from the CAA proposal [37], together with world data

needed to determine the nature of this enhancement in the cross-section.

Ideally one should perform a fine energy and angular scan of all charged and neutral pion photo-production channels. We have started just such a program, and the abundant interest in these studies is demonstrated by the recent acceptance of our CAA proposal [37] to study the  $\gamma n \rightarrow \pi^- p$  processes from the g10 data. The projected results from the CAA proposal are shown in Fig. 4. A logical continuation of this program is to study the  $\gamma p \rightarrow \pi^+ n$  process next. In the next section we describe in detail our proposed measurement of this channel.

### THE PROPOSED MEASUREMENT

We propose to carry out a measurement of the photo-pion production cross-section for the fundamental  $\gamma p \rightarrow \pi^+ n$  process from a hydrogen target at a center-of-mass energy range  $\sim 2.15$  GeV to 3.35 GeV. This measurement is to be carried out in Hall B using the CLAS detector and the tagged photon beam. The large acceptance detection and a tagged photon capabilities have enormous advantages for doing the fine energy scan and the angular scan simultaneously. We plan to perform a detailed investigation of the scaled differential cross-section  $s^7 \frac{d\sigma}{dt}$  as a function of  $\sqrt{s}$  for the  $\gamma p \rightarrow \pi^+ n$  channel up to 3.35 GeV and a detailed

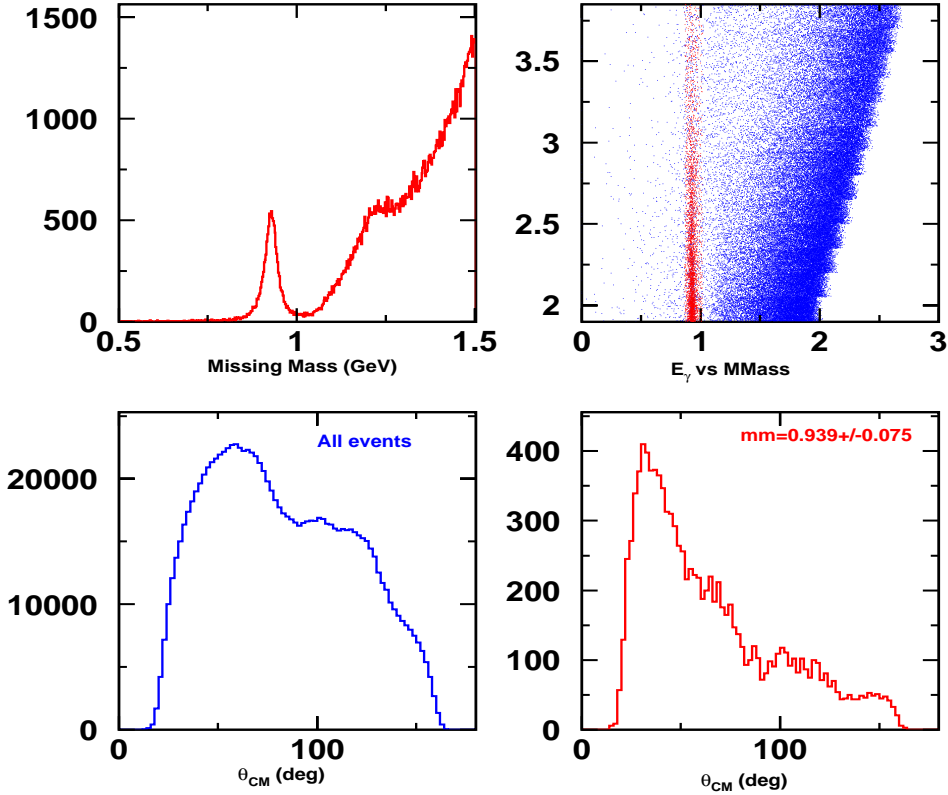


FIG. 5: Sample spectra from g11 run 44013 which had a single charge particle trigger. Upper left panel is the missing mass spectrum for  $\pi^+$  events. Upper right panel is the missing mass versus photon energy. Lower left panel is angular distribution for all pion events and lower right panel is the angular distribution for  $\gamma p \rightarrow \pi^+ n$  events.

study of the angular dependence of the scaling behavior will also be carried out. The data on the angular dependence can also be used to perform a partial wave analysis to determine the nature of the dramatic feature seen in the E94104 data for the same process. Our collaboration includes experts in partial wave analysis, for example the group from George Washington University.

For the process of interest,  $\gamma p \rightarrow \pi^+ n$ , one can use two-body kinematics to reconstruct the photon energy by detecting the  $\pi^+$  momentum and angle. The incident photon energy is known from the photon tagger. Thus, the redundancy in photon energy determination from the reconstructed photon energy based on the two-body process provides a crosscheck. This study will allow the detailed mapping of the dramatic transition region suggested by the

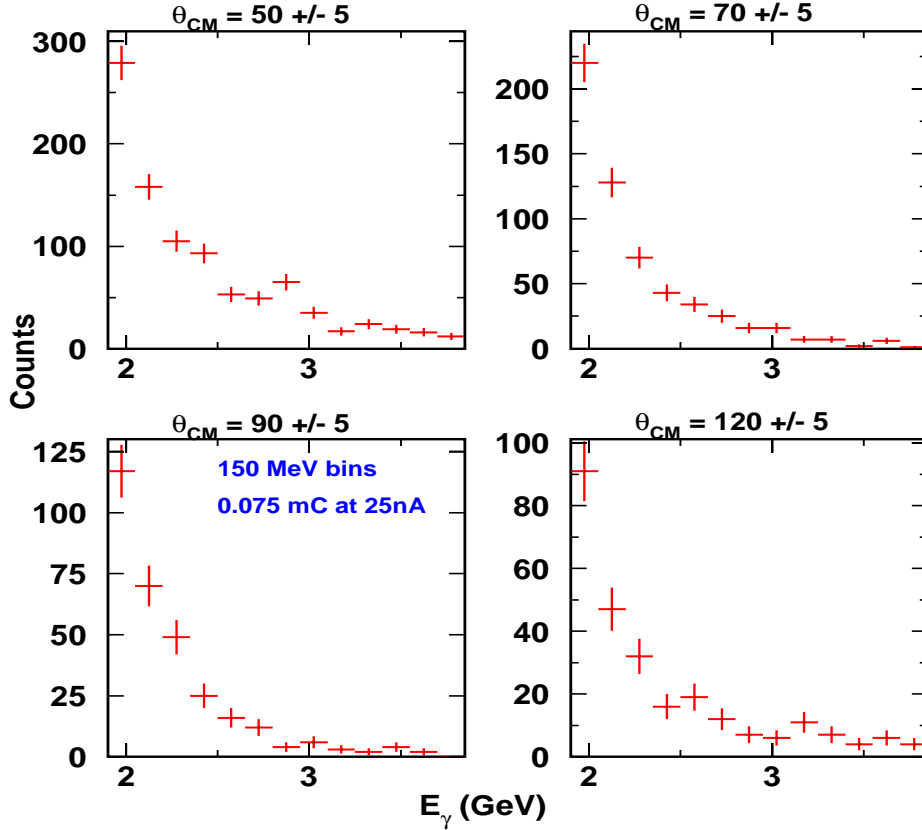


FIG. 6: Yield as function of photon energy for the  $\gamma p \rightarrow \pi^+ n$  process at  $\theta_{cm} = 50^\circ, 70^\circ, 90^\circ, 120^\circ$  obtained from a single g11 run (with single charge particle trigger).

Hall A E94-104 data [7]. It will also help confirm the oscillations in the scaled cross-section.

We have analyzed one run from the g11 running period where the trigger was set for single charged particles. This run had used a 25 nA electron beam on a 40 cm liquid hydrogen target. This gave a trigger rate of 4KHz. The sample spectra from this run are shown in Figure 5. The upper left panel shows the missing mass spectrum, where the recoiling neutron peak is clearly identifiable. The upper right panel shows a plot of photon energy versus missing mass and once again shows the neutron events (from the  $\gamma p \rightarrow \pi^+ n$  process) can be easily identified at all energies. The bottom left panel shows the broad center-of-mass angular distribution for all single pion events, while the bottom right panel shows the angular coverage for pions from the process  $\gamma p \rightarrow \pi^+ n$  (selected by putting a cut around the neutron mass in the missing mass spectrum).

Figure 6 shows the number of  $\gamma p \rightarrow \pi^+ n$  events as a function of photon energy (for 150

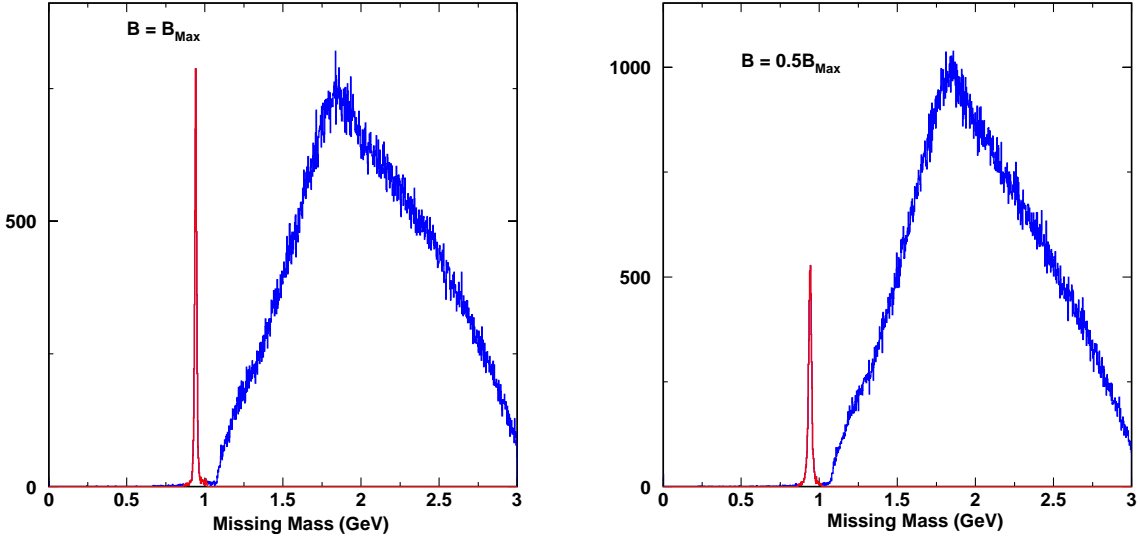


FIG. 7: The missing mass spectra from a simulation of positive pion production from hydrogen. Right panel is for  $B = 0.5 \times B_{max}$  while the left panel is for  $B = B_{max}$

MeV bins) for various  $10^\circ$  angular bins around the central C.M. angle of  $50^\circ$ ,  $70^\circ$ ,  $90^\circ$  and  $120^\circ$  respectively. These spectra are used to estimate the number of events that will be collected during the proposed experiment.

### Monte Carlo Simulation

We performed Monte Carlo simulations of the proposed experiment using the CLAS simulation package GSIM [38] and the event generator GENBOS [39]. All possible positive particle production channels for a hydrogen target were included in the event generator. The simulations were performed at  $B = B_{max}$  and at  $B = 0.5 \times B_{max}$  and compared to help decide the optimal running conditions. The results of the simulation are shown in Figures 7 - 9. Fig. 7 shows the missing mass spectrum for all positive pion events detected, it also shows (in red) the cut around the neutron mass that was used to select the  $\gamma p \rightarrow \pi^+ n$  events. The right panel is for  $B = 0.5 \times B_{max}$  while the left panel is for  $B = B_{max}$ . Fig. 8 shows the lab angle and momentum distributions of the detected pions. The panels on the left are for all detected  $\pi^+$  events while the ones on the right are for events with have a missing mass within a narrow cut around the neutron mass. The blue histograms are for

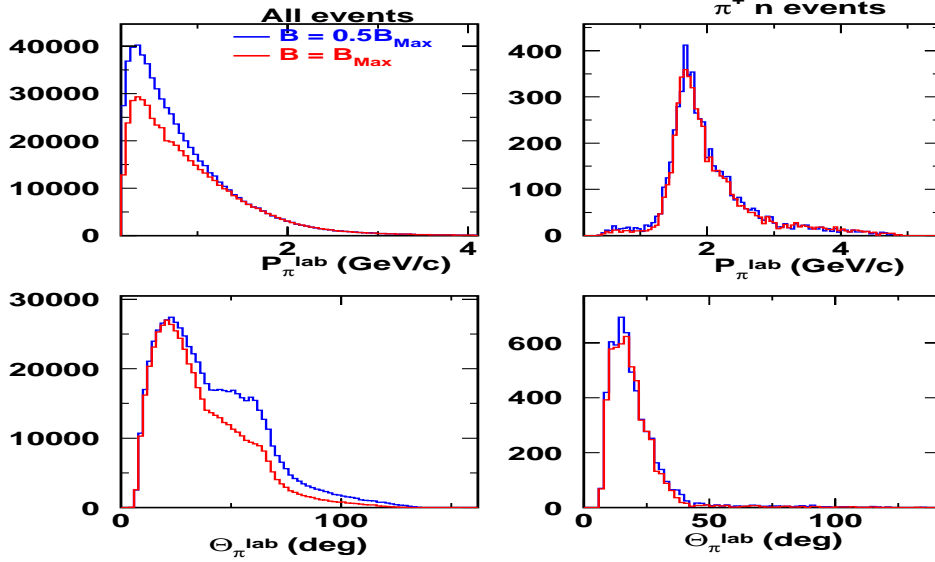


FIG. 8: The simulated lab momentum and angular distributions of events. The panels on the left are for all positive charged particle ( $\pi$ , K, P) events produced on hydrogen, while the panels on the right are for only the  $\pi^+$  events which have a missing mass around the neutron mass. The blue histograms are for  $B = 0.5 \times B_{max}$  while the red are for  $B = B_{max}$ .

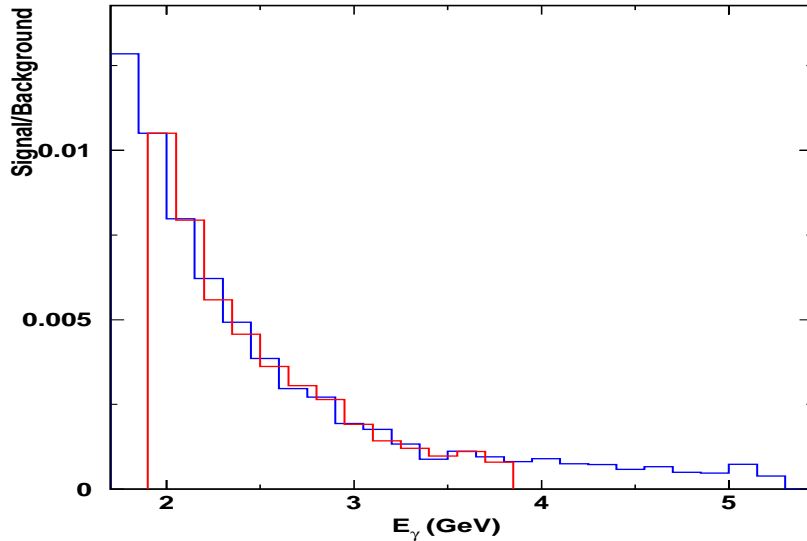


FIG. 9: The simulated signal to background ratio (blue), that was normalized to g11 data (run 44013, with single charged particle trigger) for  $E_\gamma < 3.85$  GeV shown in red.

$B = 0.5 \times B_{max}$  while the red ones are for  $B = B_{max}$ . These results clearly show that at  $B = B_{max}$  the acceptance for the background is reduced (see Fig. 7) without effecting the acceptance for the  $\gamma p \rightarrow \pi^+ n$  channel (see Fig. 8). Thus we have chosen to run this experiment at  $B = B_{max}$ . In Figure 9 we have show the simulated signal to background ratio. This ratio for  $E_\gamma < 3.85$  GeV was normalized to the data from g11 running period taken with single charged particle trigger (red histogram in Fig. 9). The simulations suggest that the signal to background is almost flat between 4 and 5.4 GeV and since one is able to separate the signal from the background at 4 GeV (as shown in Fig. 5) this experiment should be feasible.

## THE EXPERIMENT

### Overview

We propose to use the Hall B bremsstrahlung tagged photon beam and the CLAS detector with a 40 cm long cryogenic liquid hydrogen target placed at the center of CLAS. The bremsstrahlung photon beam will be produced with a gold radiator having a thickness of  $10^{-4}$  radiation lengths. We request an electron beam energy  $E_0 = 5.7$  GeV and a current of 25 nA. The entire CLAS tagger will be read out during data taking, covering from 20% to 95% of the electron beam energy, i.e.  $(1.14 \div 5.4)$  GeV. Only the portion  $(0.35 - 0.95)$  of the tagger will trigger the data acquisition, together with CLAS and the Start Counter (ST), in order to select photon energies above 2.0 GeV. Since we are interested in final states with only one charged particles we will require the detection of at least one charged particles in CLAS. Finally an in-bending torus field of  $B = B_{max}$  will be requested.

### Tagger rate

Under the above experimental conditions the rate of the entire tagger will be  $\sim 24.3 \times 10^6 \gamma/s$ . This corresponds to a rate of  $\sim 63$  kHz on each E-counter and  $\sim 400$  kHz on each T-counter. Only T-counters from 1 to 44 will be used for triggering and the corresponding rate (Master OR) going to the trigger logic will be  $\sim 15.6 \times 10^6 \gamma/s$ . The probability of multiple hits in the tagger can be estimated as

$$R_{tagger}^{multiplehits} = 2 \times \Delta\tau \times \phi_\gamma(2.0 - 5.4) \times \phi_\gamma(1.14 - 5.4) \simeq 800 \text{ kHz} \quad (2)$$

where the time coincidence of  $\Delta\tau = 1$  ns reflects the time resolution achievable in the off-line analysis. This rate corresponds to  $\sim 5\%$  of the MOR rate and it is an acceptable value. In addition, most of these events will be recoverable in the final analysis since typically one of the two photons will have an energy which is not compatible with the total energy observed in the detector. In doing this task we will also be helped by our two-body kinematics.

### CLAS, Start Counter and MOR: Trigger rates and accidentals

The relevant hadronic rate comes from photons (mainly untagged) above the pion threshold ( $E_\gamma > 140$  MeV) which corresponds to  $58 \times 10^6 \gamma/s$ . This means that, assuming a photo-absorption cross section of  $\sigma_{hadron} = 150 \mu\text{barn}$

$$R_{hadron} = \phi_\gamma(E_\gamma > \pi) \cdot T_{length} \cdot \rho \cdot N \cdot \sigma_{hadron} \simeq 15 \text{ kHz} \quad (3)$$

where  $T_{length} = 40$  cm is the target length,  $N = 6.02 \times 10^{23}$  is the Avogadro's number and  $\rho = 0.0708 \text{ gr/cm}^3$  is the liquid hydrogen density. Approximately 28% of these events comes from photons with energy above 2 GeV, 16% from photons between 1.14 and 2 GeV and the remaining 56% from untagged photons. All these events will produce a hit in the Start Counter, which is almost 100% of acceptance, while CLAS will see only  $\sim 60\%$  of them (we have evaluated this number considering  $\sim 90\%$  for the single particle detection efficiency and  $\sim 70\%$  for the CLAS acceptance).

In addition to the hadronic events, the Start Counter will also be affected by the electromagnetic background produced by the photon beam. Based on the work of [40] and from g11 experiment, this electromagnetic background could be estimate of the order of  $\sim 7$  MHz. To estimate the trigger rate and the accidentals we will proceed in two steps: first we will consider the MOR x ST coincidence rate and then the (MOR x ST) x CLAS one.

- MOR x ST

To select photons with energy above 2 GeV, the MOR will be used in coincidence with the Start Counter within a 10 ns coincidence window. The MOR x ST coincidence rate will be affected by two type of accidentals:

- 1) Hadronic events in the Start Counter induced by photons which are below the minimum triggered energy of 2 GeV;
- 2) hits in the Start Counter induced by electromagnetic background.

Assuming a coincidence window of  $\Delta\tau = 10$  ns, we have:

$$R_{MORXST}^{acc1} = 2 \cdot \Delta\tau \cdot \phi_{tagged} \cdot (R_{ST}^{hadr} - R_{ST}^{hadr}(tagged)) \simeq 3.4 \text{ kHz} \quad (4)$$

where  $R_{ST}^{hadr} = 15$  kHz

$$R_{MORXST}^{acc2} = 2 \cdot \Delta\tau \cdot \phi_{tagged} \cdot R_{ST}^{BG} \simeq 370 \text{ kHz} \quad (5)$$

where for  $R_{ST}^{BG}$  a value of 1.2 MHz has been chosen. In fact, the segmentation of the new Start Counter allows for a configuration in which groups of 6 scintillators could be put in coincidence with each CLAS sector. Thus the total 7 MHz has been divided by 6.

- MOR x ST x CLAS

After requiring the coincidence with CLAS, the first accidental rate will be reduced by the CLAS acceptance and efficiency while, on the contrary, the second rate will be reduced to a much greater extent, since it is uncorrelated with CLAS.

Assuming a coincidence window  $\Delta\tau = 100$  ns, the final accidental rates are estimated to be:

$$R_{(MORXST)XCLAS}^{acc1} = R_{MORXST}^{acc1} \cdot Eff_{CLAS} \simeq 2 \text{ kHz} \quad (6)$$

$$R_{(MORXST)XCLAS}^{acc2} = 2 \cdot \Delta\tau \cdot R_{MORXST}^{acc2} \cdot (R_{ST}^{hadr} - R_{ST}^{hadr}(tagged)) \cdot Eff_{CLAS} \simeq 490 \text{ Hz} \quad (7)$$

The total DAQ rate is then:

$$R_{trigger} = R_{hadr}^{true} \cdot Eff_{CLAS} + R_{(MORXST)XCLAS}^{acc1} + R_{(MORXST)XCLAS}^{acc2} \simeq 4.4 \text{ kHz} \quad (8)$$

which is within the DAQ limits.

In the off-line data analysis the "true" events will be extracted from the total recorded events using a tighter time coincidence between Start Counter and MOR. This software coincidence window is set to 1 ns and will reduce the accidental rate to  $\simeq 200$  Hz and to  $\simeq 48$  Hz respectively.

The final contamination to the true rate due to accidentals is therefore estimated to be less than 10%.

## Counting Rates and Beam Time Estimate

Based on the sample spectra obtained from run 44013 of the g11 running period, we can estimate the number of events we can expect to get in 100 hours of running with a 25 nA beam on a 40 cm liquid hydrogen target. We have estimated the expected yield for 10° bins around the C.M. angles of 50°, 70°, 90° and 120°. The yield is determined for each photon energy bin (150 MeV wide) based on the rates shown in Figure 6. For photon energy beyond 3.8 GeV the yield is estimated by assuming  $s^{-7}$  scaling. These rates were found to be consistent with the rates measured in the previous experiment (E94104) at 70° and 90°. For the 50° case however, it is clear that the scaling assumption under-estimates the yields.

We have also carried out a preliminary study of the feasibility of running the proposed experiment concurrently with the g12 experiments. There are in principle two possibilities: (1) running with an additional single charged particle trigger with a prescaling factor; (2) adding a second trigger with one charged particle in CLAS and one neutral particle in the opposite sector from the Electromagnetic Calorimeter (EC + LAC). For the proposed experiment, precise knowledge of the photon flux is crucial for the extraction of the differential cross-section. Therefore, we want to avoid multiple triggers because of the potential ambiguities in determination of the photon flux. There are also potential issues both in the extraction of cross-section from prescaled data, and in the determination of the neutral particle detection and trigger efficiencies.

Therefore, our conclusion is to request for 4 days of dedicated beam time for the proposed experiment with a current of 25 nA and a beam energy of 5.7 GeV with a dedicated single charged particle trigger in CLAS. We would like to run this experiment following the g12 running to minimize the overhead needed for running this experiment.

## Projected Results

The expected coverage in the center of mass energy  $\sqrt{s}$  and angle  $\theta_{CM}$  are shown in Figure 10. The projected results for  $\theta_{cm}$  centered around 90°, 70° and 50°, are shown in Figure 11. Only the statistical uncertainties are shown in these projections.

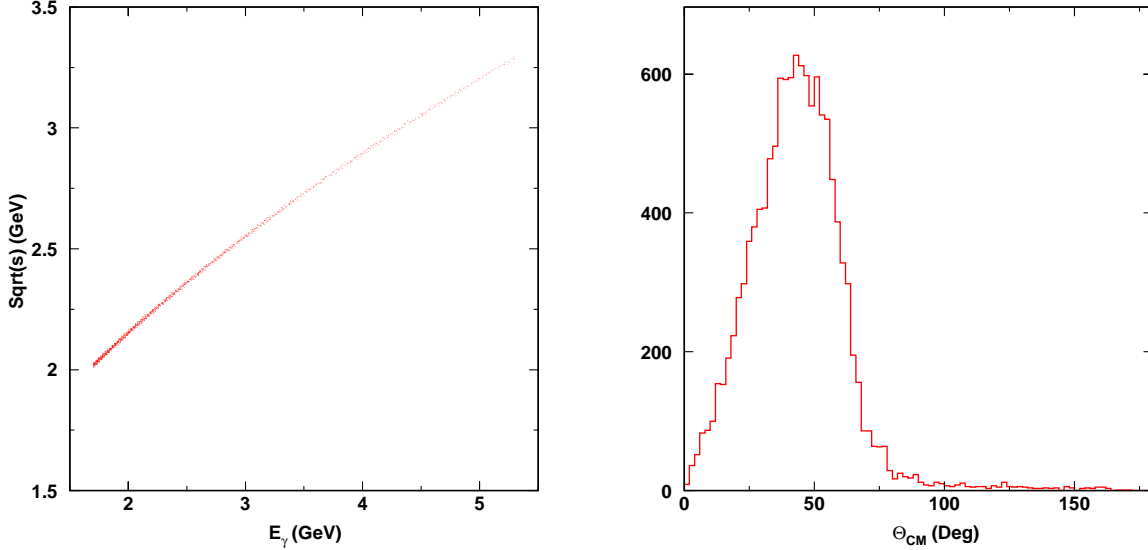


FIG. 10: The center of mass energy  $\sqrt{s}$  vs the incident photon energy for the simulated  $\gamma p \rightarrow \pi^+ n$  events (left). The simulated coverage of the pion center of mass angle (right).

### SUMMARY

We have proposed a measurement of the  $\gamma p \rightarrow \pi^+ n$  reaction using the CLAS detector. With an energy beam of  $E_0 = 5.7$  GeV we plan to map out the region of  $\sqrt{s} = 2.15 - 3.35$  GeV in fine steps of approximately 0.15 GeV and also perform an angular scan in steps of  $10^\circ$ . These measurements would i) provide information on the onset of scaling behavior over a wide angular range, ii) help understand the dramatic enhancement and rapid drop in the scaled cross-section observed in the E94104 data and iii) test the possible oscillatory behavior of the scaled free space differential cross-sections about the quark counting prediction. We will use the standard Hall B equipment along with the radiator and tagger. The Hall B cryogenic 40 cm liquid hydrogen target will be used. A total of 100 hours (4 days) of beam time will be required for this experiment.

### ACKNOWLEDGMENTS

We thank R. Schumacher for providing preliminary results on the  $\gamma p \rightarrow \pi^+ n$  from the glc data, and M. Dugger and B. Ritchie for providing data on the  $\gamma p \rightarrow \pi^0 p$  process. We also thank P. Eugenio, B. Mecking, S. Stepanyan, P. Stoler, and D. Weygand for helpful

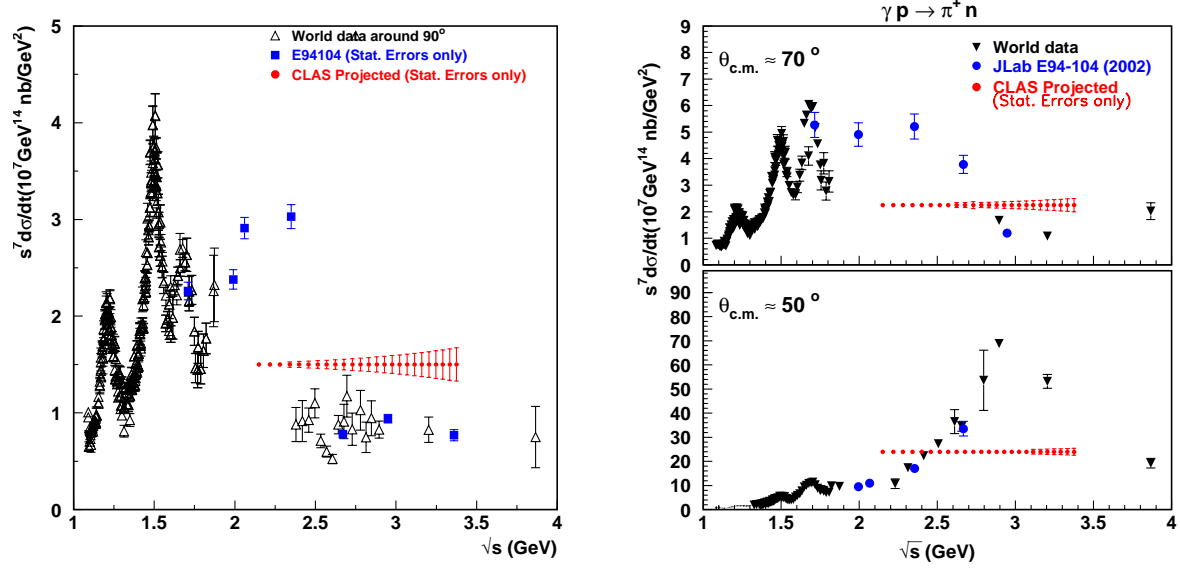


FIG. 11: Projected results for the  $\gamma p \rightarrow \pi^+ n$  process at  $\theta_{cm} = 90^\circ$  (left panel) and projected results for the  $\gamma p \rightarrow \pi^+ n$  process at  $\theta_{cm} = 70^\circ$  and  $50^\circ$  (right panel).

discussions.

- 
- [1] S.J. Brodsky and G.R. Farrar, Phys. Rev. Lett. **31**, 1153 (1973); Phys. Rev. D **11**, 1309 (1975); V. Matveev *et al.*, Nuovo Cimento Lett. **7**, 719 (1973);
- [2] R. L. Anderson *et al.*, Phys. Rev. D **14**, 679 (1976); C. White *et al.*, Phys. Rev. **D49**, 58 (1994).
- [3] J. Napolitano *et al.*, Phys. Rev. Lett. **61**, 2530 (1988); S.J. Freedman *et al.*, Phys. Rev. C **48**, 1864 (1993); J.E. Belz *et al.*, Phys. Rev. Lett. **74**, 646 (1995).
- [4] C. Bochna *et al.*, Phys. Rev. Lett. **81**, 4576 (1998).
- [5] E.C. Schulte, *et al.*, Phys. Rev. Lett. **87**, 102302 (2001);
- [6] P. Rossi *et al.*, Phys. Rev. Letts. **94**, 012301 (2005); M. Mirazita *et al.*, Phys. Rev. C **70**, 014005 (2004).
- [7] L. Y. Zhu *et al.*, Phys. Rev. Lett. **91**, 022003 (2003); L. Y. Zhu *et al.* Phys Rev. C, **71**, 044603 (2005).
- [8] K. Wijesooriya, *et al.*, Phys. Rev. Lett. **86**, 2975 (2001).
- [9] H. Genzel, P. Joos, and W. Pfeil, Photoproduction of Elementary Particles (Springer-Verlag,

- Berlin, 1973), Group I Volume 8 of Numerical Data and Functional Relationships in Science and Technology, edited by K.-H. Hellwege.
- [10] O. Bartholomy *et al.*, Phys. Rev. Lett. **94**,012003 (2005).
  - [11] R.L. Anderson *et al.*, Phys. Rev. **D14**, 679 (1976).
  - [12] H.-J. Besch *et al.*, Z. Phys. C **16**, 1 (1982).
  - [13] I. I. Strakovsky (private communication); R. A. Arndt *et al.*, Phys. Rev. **C66**, 055213 (2002); nucl-th/0205067; <http://gwdac.phys.gwu.edu/>.
  - [14] I. I. Strakovsky (private communication); S. S. Kamalov, *et al.*, Phys. Rev. C **64**, 032201 (2001)(A dynamical model); D. Drechsel, *et al.*, Nucl. Phys. A **645**, 145 (1999)(a unitary isobar model); MAID2001 refers to the Nov. 2001 version of the MAID solution from S. S. Kamalov.
  - [15] P. V. Landshoff, Phys. Rev. D **10**, 1024 (1974).
  - [16] J. Polchinski and M.J. Strassler, Phys. Rev. Lett. **88**, 031601 (2002); R.C. Brower and C.I. Tan, Nucl. Phys. B **662**, 393 (2003); O. Andreev, Phys. Rev. D **67**, 046001 (2003).
  - [17] N. Isgur and C. Llewelyn-Smith, Phys. Rev. Lett. **52**, 1080 (1984).
  - [18] A.W. Hendry, Phys. Rev. D **10**, 2300 (1974).
  - [19] D.G. Crabb *et al.*, Phys. Rev. Lett. **41**, 1257 (1978).
  - [20] G.R. Court *et al.*, Phys. Rev. Lett. **57**, 507 (1986), T.S. Bhatia *et al.*, Phys. Rev. Lett. **49**, 1135 (1982), E.A. Crosbie *et al.*, Phys. Rev. D **23**, 600 (1981).
  - [21] S.J. Brodsky, C.E. Carlson, and H. Lipkin, Phys. Rev. D **20**, 2278 (1979).
  - [22] J.P. Ralston and B. Pire, Phys. Rev. Lett. **61**, 1823 (1988), J.P. Ralston and B. Pire, Phys. Rev. Lett. **65**, 2343 (1990).
  - [23] C.E. Carlson, M. Chachkhunashvili, and F. Myhrer, Phys. Rev. D **46**, 2891 (1992).
  - [24] S. J. Brodsky, and G. F. de Teramond, Phys. Rev. Lett. **60**, 1924 (1988).
  - [25] Q. Zhao and F. E. Close, Phys. Rev. Lett. **91**, 022004 (2003).
  - [26] X. Ji, J.-P. Ma and F. Yuan, Phys. Rev. Lett. **90**, 241601 (2003).
  - [27] S. J. Brodsky and G. F. de Teramond, Phys. Lett. **B582**, 211 (2004); S. J. Brodsky *et al.*, Phys. Rev. D **69**, 076001 (2004).
  - [28] L.L. Frankfurt, G.A. Miller, M.M. Sargsian, and M.I. Strikman, Phys. Rev. Lett. **84**, 3045 (2000), M.M. Sargsian, private communication.
  - [29] P. Jain, B. Kundu, and J. Ralston, hep-ph/0005126.
  - [30] G.R. Farrar, G. Sterman, and H. Zhang, Phys. Rev. Lett. **62**, 2229 (1989).

- [31] E. Anciant *et al.*, Phys. Rev. Lett. **85**, 4682 (2000).
- [32] R. Schumacher, private communication.
- [33] M. Dugger, B. Ritchie, private communication; The Bonn data from CB-ELSA is from O. Bartholomy *et al.*, Phys. Rev. Lett **94**, 012003 (2005)
- [34] S. Capstick, Phys. Rev. D **46**, 2864 (1992); S. Capstick and W. Roberts, Phys. Rev. D **49**, 4570 (1994).
- [35] S.J. Brodsky, I.A. Schmidt, G.F. de Teramond, Phys. Rev. Lett. **64**, 1011 (1990).
- [36] H. Gao, T.S.-H. Lee, and V. Marinov, Phys. Rev. C **63**, 022201(R) (2001).
- [37] CLAS Approved Analysis; *Single charged pion photoproduction  $\gamma n \rightarrow \pi^- p$  on deuterium*, D. Dutta, H. Gao and P. Rossi spokespersons, June (2005).
- [38] M. Guidal *et al.*, CLAS-note 93-013
- [39] A. S. Iljinov *et al.*, Nucl. Phys. A **616**, 575 (1997)
- [40] M. Guidal *et al.*, CLAS-note 95-009.